

**UNSTEADY INCOMPRESSIBLE FLOW AND HEAT TRANSFER OF DUSTY
NON-IONIZED FLUID WITH CHARGED SUSPENDED PARTICULATE MATTER
(SPM) BETWEEN TWO INFINITE PARALLEL PLATES DUE TO THE MOTION OF
ONE OF THEM**

Misra A.^{1*} and Prakash J.²

*Author for correspondence

¹Department of Mathematics, Centurion University of Technology and Management,
Paralakhemundi, Gajapati (Orissa), India
Email: ashok.misra@jitm.org

²Department of Mathematics, Faculty of Science, University of Botswana,
Private Bag 0022, Gaborone, Botswana
Email: prakashj@mopipi.ub.bw

ABSTRACT

In the study of transport phenomena, mass, momentum and energy are increasingly recognized of fundamental importance. The prediction of the mechanical transport in the ocean is a difficult task. Parallel flow through a straight channel provides a good understanding in connection with flow in estuaries. Thus to study the transport through estuaries, a simple case of an unsteady incompressible flow and heat transfer of a non-ionized fluid with charged SPM between two infinite parallel plates has been considered. The solutions of the governing equations of flow field have been obtained by using Crank-Nicholson finite difference technique. An illustration of dependence of physical variables on non-dimensional parameters viz. diffusion parameter, finite volume fraction, concentration parameter, magnetic parameter has been depicted through figures and tables. The direction of heat transfer has been discussed by taking a situation $P_r E_c \geq < 2$ in both frozen flow and equilibrium flow regimes. The electrification of particles has an effect on reduction of the velocity of carrier fluid as well as SPM but on increase of the temperature of carrier fluid and SPM.

INTRODUCTION

There have been several investigations of Couette flow of dusty fluid. Saffman [1] has formulated the basic equations for the flow of dusty fluid and has presented the modified form of Navier-Stokes equations for the fluid and the particle phases. Michael and Miller [2] have studied the flow

produced by the motion of an infinite plane in a steady dusty gas occupying the semi-infinite space above it. Later, Baral [3] has discussed the plane parallel flow of conducting dusty gas. Jana and Datta [4] have studied Couette flow and heat transfer in a rotating system and have found closed form solutions to study heat transfer characteristics. Nag *et al.* [5] have studied the Couette flow of a dusty gas between two parallel infinite plates for impulsive start as well as for uniformly accelerated start of one of the plates and have found the solution of the problem with the help of Laplace transform technique. Mitra and Bhattacharyya [6] have studied the unsteady hydromagnetic laminar flow of a conducting dusty fluid between two parallel plates started impulsively from rest. Datta and Mishra [7] have studied unsteady Couette flow and heat transfer of a dusty fluid filling the gap between two infinite parallel plates kept at arbitrary temperature and found the solution to be valid for any time by using Laplace transform followed by its Numerical Inversion. Datta and Mishra [8] have studied Couette flow of a dusty fluid in a rotating frame of reference for impulsive start as well as for uniformly accelerated start of one of the plates by using Laplace transform technique followed by Numerical inversion. Aboul-Hassan *et al.* [9] have studied the temperature distribution in a dusty conducting fluid flowing through two parallel infinite plates due to the motion of one of the plates. Panda *et al.* [10] have studied the unsteady Couette flow and heat transfer of a dusty fluid with the inclusion of volume fraction and Brownian

diffusion of SPM in the mathematical formulation. They have obtained the solution by using Crank-Nicholson finite implicit scheme. Attia [11] has studied the unsteady Couette flow and heat transfer of a dusty conducting fluid between two parallel plates with variable viscosity and electric conductivity. He has obtained the solution numerically using finite differences. Govindarajan *et al.* [12] have investigated the three dimensional couette flow of dusty viscous fluid with transpiration cooling by applying the transverse sinusoidal injection at the stationary plate and constant suction at the moving plate. Gireesha *et al.*[13] have studied the unsteady laminar flow of an electrically conducting viscous incompressible fluid with embedded non-conducting identical spherical particles bounded by two infinite flat plates under the influence of a uniform magnetic field and have obtained the solution of the problem with the help of Laplace transform technique. Attia [14] has studied the unsteady Couette flow and heat transfer of a dusty conducting fluid between two parallel plates with temperature dependent viscosity and thermal conductivity. The fluid is acted upon by an exponential decaying pressure gradient under an applied external uniform magnetic field. He has solved the coupled momentum and energy equations numerically using finite differences. Eguía *et al* [15] have investigated the effects of dependence on temperature of the viscosity and electric conductivity, Reynolds number and particle concentration on the unsteady MHD flow and heat transfer of a dusty, electrically conducting fluid between parallel plates in the presence of an external uniform magnetic field using the network simulation method (NSM).

In most of the theoretical and experimental studies of the flow of dusty fluids between two infinite parallel plates, the volume fraction of suspended particles, the diffusion of particles through carrier fluid and also the effect of charged suspended particulate matter have been neglected. But consideration of finite volume fraction in flow analysis is well justified at high fluid density and at high particle mass fraction. The random motion of the SPM must be taken into account for all practical purposes. Again Loeb [16] and Soo [17] have described that a very slight charge on solid particles has a significant effect on concentration distribution in the flow of a gas-solid system. Contribution of charges on the solid particles to dynamics of a gas-solid suspension includes elementary relations of electrostatics and electrodynamics.

In this study, the finite volume fraction, Brownian diffusion and electrification of SPM are considered in a non-ionized incompressible fluid to show their effects

on the unsteady flow and heat transfer between two infinite parallel plates due to the motion of one of them.

NOMENCLATURE

p	Pressure of fluid phase
h	Distance between two parallel plates
t	Time
(x, y, z)	Space coordinates
ρ_{p_∞}	Density of the particles in the free stream
(u, v, w)	Velocity components of fluid phase
(u_p, v_p, w_p)	Velocity components of particle phase
(F_x, F_y, F_z)	Components of the force due to electrification of particles
U	Free stream velocity
\vec{V}, \vec{V}_p	Velocity vectors of fluid & particle phases respectively
T	Temperature of fluid phase
T_p	Temperature of particle phase
T_o, T_h	Temperatures of the lower & upper plates respectively
C_{f_0}, C_{f_1}	Skin friction coefficients at the lower and upper plates respectively
Re	Fluid phase Reynolds number
(θ, θ_p)	Non-dimensional temperature of fluid and particle phases respectively
Ec	Eckret number
Pr	Prandtl number
(ρ, ρ_p)	Densities of fluid and particle phases respectively
(μ, μ_p)	Coefficients of viscosities of fluid and particle phases
(ν, ν_p)	Kinematic coefficient of viscosities of fluid and particle phases respectively
N_u	Nusselt number
K	Thermal conductivity
E	Electric field intensity
J	Current density
B_0	Constant field intensity ($= \mu_e H_0$)
H_0	Constant field strength
\vec{F}_e	Force due to electrification of charged SPM
M	Magnetic number
α	Concentration parameter (ρ_p/ρ)
U	Free stream velocity
σ	Electrical conductivity of the medium
J^2/σ	Energy source due to magnetic field
η	Dimensionless co-ordinate

	perpendicular to the plate
μ_e	Magnetic permeability
ε	Diffusion parameter (ν_p/ν)
ρ_s	Density of the material of the particle
ϕ	Volume fraction of the suspended particles
τ_w	Skin friction
γ	Ratio of specific heats (C_s/C_p)
λ	Velocity equilibration length
B	Electromagnetic field intensity
Λ	Non-dimensional velocity Relaxation length

FORMULATION OF THE PROBLEM & SOLUTION

Consider the motion of a fluid with uniformly distributed electrified dust particles filling the gap between two infinite insulated parallel plates. At time $t < 0$ both the fluid and the plates are assumed to be at rest. At $t = 0$ the upper plate begins to move impulsively in its own plane with a velocity U , while lower plate, at a distance h apart remains fixed. The lower and upper plates are maintained at uniform temperature T_0 and T_h respectively.

A Cartesian coordinate system has been chosen with x -axis along the lower plate and in the direction of motion, y -axis perpendicular to it and z -axis lying on the lower plate. It is assumed that the intensity \vec{B} of the magnetic field of constant strength H_0 is acting in the direction of y -axis and fixed relative to it. Magnetic permeability μ_e is constant throughout the field. The electric field $\vec{E} = 0$ as there exist no applied or polarization voltage.

In the present problem the components of \vec{V} , \vec{V}_p , \vec{B} , \vec{E} are given by:

$$\vec{V} = (u, 0, 0); \vec{V}_p = (u_p, 0, 0); \vec{B} = (0, B_0, 0); \vec{E} = (0, 0, 0)$$

The Lorentz force \vec{F}_e due to electrification of SPM has the components $\vec{F}_e = (-\sigma B_0^2 u_p, 0, 0)$

and the energy source due to the magnetic field $= \frac{J^2}{\sigma} = \sigma B_0^2 u_p^2$

Now the governing equations of flow field for unsteady incompressible non-ionized fluid with charged SPM after using the non-dimensional variables are given by:

$$\frac{\partial \rho_p}{\partial t} = \varepsilon \frac{\partial^2 \rho_p}{\partial \eta^2} \quad (1)$$

$$(1-\phi) \frac{\partial u}{\partial t} = \frac{\partial^2 u}{\partial \eta^2} + \frac{\rho_p \alpha R_e}{\Lambda} (u_p - u) \quad (2)$$

$$\phi \frac{\partial u_p}{\partial t} = \frac{R_e}{\Lambda} (u - u_p) - \varepsilon \frac{\partial^2 u_p}{\partial \eta^2} - M \frac{u_p}{\rho_p} \quad (3)$$

$$(1-\phi) \frac{\partial \theta}{\partial t} = \frac{1}{P_r} \left(\frac{\partial^2 \theta}{\partial \eta^2} \right) + \frac{2}{3} \frac{\rho_p \alpha R_e}{P_r \Lambda} (\theta_p - \theta) + E_c \left(\frac{\partial u}{\partial \eta} \right)^2 + \frac{\rho_p \alpha R_e E_c}{\Lambda} (u_p - u)^2 \quad (4)$$

$$\phi \frac{\partial \theta_p}{\partial t} = \frac{2}{3} \frac{R_e}{\gamma P_r \Lambda} (\theta - \theta_p) - \frac{\varepsilon E_c}{\gamma} \left[u_p \frac{\partial^2 u_p}{\partial \eta^2} + \left(\frac{\partial u_p}{\partial \eta} \right)^2 \right] + \frac{M \cdot E_c}{\gamma} \frac{u_p^2}{\rho_p} \quad (5)$$

The initial and boundary conditions for this problem are:

$$\left. \begin{aligned} u = u_p = 0 \text{ in } 0 \leq \eta \leq 1 \text{ for } t \leq 0 \\ u = 0, \theta = 0 \text{ at } \eta = 0 \text{ for } t > 0 \\ u = 1, \theta = 1 \text{ at } \eta = 1 \text{ for } t > 0 \end{aligned} \right\} \quad (6)$$

Employing Crank-Nicholson finite implicit scheme, equations (1) to (5) are reduced to the following forms:

$$-A_i \rho_{p_{i-1,n+1}} + B_i \rho_{p_{i,n+1}} - C_i \rho_{p_{i+1,n+1}} = D_i \quad (7)$$

$$-A_i u_{i-1,n+1} + E_i u_{i,n+1} - C_i u_{i+1,n+1} = F_i \quad (8)$$

$$-A_i u_{p_{i-1,n+1}} + E_{p_i} u_{p_{i,n+1}} - C_i u_{p_{i+1,n+1}} = F_{p_i} \quad (9)$$

$$-A_i \theta_{i-1,n+1} + G_i \theta_{i,n+1} - C_i \theta_{i+1,n+1} = H_i \quad (10)$$

$$\theta_{p_{i,n+1}} = \frac{BB \theta_{p_{i,n}} + R D_i}{DD}; i = 0, N \quad (11)$$

Where, $A_i = 1$; $B_i = 2 + \frac{2\lambda}{\varepsilon}$; $C_i = 1$; $\lambda = \frac{\Delta\eta^2}{\Delta t}$;

$$D_i = \rho_{p_{i-1,n}} + \left(-2 + \frac{2\lambda}{\varepsilon}\right) \rho_{p_{i,n}} + \rho_{p_{i+1,n}};$$

$$E_i = 2 + \frac{\alpha R_e \Delta\eta^2 \rho_{p_{i,n+1}}}{\Lambda} + 2(1-\phi)\lambda;$$

$$E_{\rho_i} = \left(2 - \frac{R_e \Delta\eta^2}{\Lambda \varepsilon} - \frac{2\phi\lambda}{\varepsilon} - \frac{M \Delta\eta^2}{\varepsilon \rho_{p_{i,n+1}}}\right);$$

$$F_i = u_{i-1,n} + \left(2(1-\phi)\lambda - 2 - \frac{\alpha R_e \Delta\eta^2 \rho_{p_{i,n+1}}}{\Lambda}\right) u_{i,n} + u_{i+1,n} \\ + \frac{2\alpha R_e \Delta\eta^2 \rho_{p_{i,n+1}}}{\Lambda} u_{p_{i,n}};$$

$$F_{\rho_i} = u_{p_{i-1,n}} + \left(\frac{R_e \Delta\eta^2}{\Lambda \varepsilon} - 2 - \frac{2\phi\lambda}{\varepsilon} + \frac{M \Delta\eta^2}{\varepsilon \rho_{p_{i,n+1}}}\right) u_{p_{i,n}} \\ + u_{p_{i+1,n}} - \frac{2R_e \Delta\eta^2}{\varepsilon \Lambda} u_{i,n+1};$$

$$G_i = 2 + \frac{2\alpha R_e \Delta\eta^2 \rho_{p_{i,n+1}}}{3\Lambda} + 2(1-\phi)P_r \lambda;$$

$$B B = \phi\lambda - \frac{R_e \Delta\eta^2}{3 \gamma P_r \Lambda};$$

$$H_i = \theta_{i-1,n} + \left(-2 - \frac{2\alpha R_e \Delta\eta^2 \rho_{p_{i,n+1}}}{3\Lambda} + 2(1-\phi)P_r \lambda\right) \theta_{i,n} + \theta_{i+1,n} \\ + \frac{4\alpha R_e \Delta\eta^2 \rho_{p_{i,n+1}}}{3\Lambda} \theta_{p_{i,n}} + 2E_c P_r (u_{i+1,n+1} - u_{i,n+1})^2 \\ + \frac{2\alpha E_c . R_e P_r \Delta\eta^2 \rho_{p_{i,n+1}}}{\Lambda} (u_{p_{i,n+1}} - u_{i,n+1})^2;$$

$$D D = \phi\lambda + \frac{R_e \Delta\eta^2}{3 \gamma P_r \Lambda};$$

$$R D_i = \frac{2R_e \Delta\eta^2}{3\gamma P_r \Lambda} \theta_{i,n+1} - \frac{\varepsilon E_c}{\gamma} (u_{p_{i+1,n+1}} - u_{p_{i,n+1}})^2 \\ + \frac{M . E_c \Delta\eta^2}{\gamma} \frac{u_{p_{i,n+1}}^2}{\rho_{p_{i,n+1}}} - \frac{\varepsilon E_c u_{p_{i,n+1}}}{\gamma} (u_{p_{i+1,n+1}} - 2u_{p_{i,n+1}} + u_{p_{i-1,n+1}})$$

As no slip condition is not satisfied by the particles, so the compatibility conditions at the plates are considered for ρ_p and u_p .

Using the compatibility condition at lower and upper plates for ρ_p

$$\left. \frac{\partial \rho_p}{\partial t} \right|_{\eta=0,1} = \varepsilon \left. \frac{\partial^2 \rho_p}{\partial \eta^2} \right|_{\eta=0,1}$$

we obtain for $i = 0$, $\rho_{p_{0,n+1}} = 2\rho_{p_{0,n}} - \rho_{p_{0,n-1}}$

and for $i = N$, $\rho_{p_{N,n+1}} = 2\rho_{p_{N,n}} - \rho_{p_{N,n-1}}$

Similarly using the compatibility condition at lower and upper plates for u_p

$$\phi \left. \frac{\partial u_p}{\partial t} \right|_{\eta=0,1} = \frac{R_e}{\Lambda} (u - u_p) \Big|_{\eta=0,1} - \varepsilon \left. \frac{\partial^2 u_p}{\partial \eta^2} \right|_{\eta=0,1} - M \frac{u_p}{\rho_p} \Big|_{\eta=0,1}$$

we obtain for $i = 0$,

$$u_{p_{0,n+1}} = \left[2 + \frac{M . \Delta t}{\phi} \left\{ \frac{1}{\rho_{p_{0,n}}} - \frac{1}{\rho_{p_{0,n+1}}} \right\}\right] u_{p_{0,n}} - u_{p_{0,n-1}} + \frac{R_e . \Delta t}{\phi \Lambda} [u_{0,n+1} - u_{0,n}]$$

and for $i = N$,

$$u_{p_{N,n+1}} = \left[2 + \frac{M . \Delta t}{\phi} \left\{ \frac{1}{\rho_{p_{N,n}}} - \frac{1}{\rho_{p_{N,n+1}}} \right\}\right] u_{p_{N,n}} - u_{p_{N,n-1}} + \frac{R_e . \Delta t}{\phi \Lambda} [u_{N,n+1} - u_{N,n}]$$

HEAT TRANSFER

The heat transfer characteristic is expressed in terms of the Nusselt number, defined as

$$N_u = \frac{h (q_{w_1} - q_{w_0})}{K (T_h - T_0)}$$

Where q_{w_0} and q_{w_1} represent the rates of heat transfer per unit area at the plates $y = 0$ and $y = h$ respectively and are given by

$$q_{w_0} = -K \frac{\partial T}{\partial \eta} \cdot \frac{\partial \eta}{\partial y} \Big|_{\eta=0} ; \quad q_{w_1} = -K \frac{\partial T}{\partial \eta} \cdot \frac{\partial \eta}{\partial y} \Big|_{\eta=1}$$

DISCUSSION OF RESULTS AND CONCLUSION

From Tables 1 to 3 the following typical results have been observed. In frozen flow regime, which refers to small times, the heat is transferred from lower plate to fluid, fluid to upper plate and the Nusselt number remains positive indicating that the heat transfers from fluid to upper plate for all values of $P_r E_c \geq < 2$. In the equilibrium flow regime, which refers to large times, heat flows from upper plate to fluid, fluid to lower plate and the Nusselt number remains negative indicating that the heat transfers from upper plate to fluid for all values of $P_r E_c \geq < 2$.

Table - 1 $P_r = 0.72$, $E_c = 0.05$ ($P_r E_c < 2$)

t	q_{w_0}	q_{w_1}	N_u
0.0075	2.010	-24.645	26.655
0.0175	2.018	-21.880	23.898
0.0225	2.020	-19.070	21.090
0.2525	-2.285	25.415	-27.735
0.4325	-4.820	27.740	-32.560
0.4775	-5.570	28.310	-33.880

Table - 2 $P_r = 0.72$, $E_c = 2.77$ ($P_r E_c \approx 2$)

t	q_{w_0}	q_{w_1}	N_u
0.0075	2.595	-27.665	30.260
0.0175	2.920	-20.985	23.905
0.0225	3.050	-16.375	19.425
0.2525	-3.215	13.500	-16.715
0.4325	-5.120	15.715	-20.835
0.4775	-6.460	17.440	-23.900

Table - 3 $P_r = 0.72$, $E_c = 4.16$ ($P_r E_c > 2$)

t	q_{w_0}	q_{w_1}	N_u
0.0075	2.895	-29.870	32.765
0.0175	3.380	-27.190	30.570
0.0225	3.580	-15.000	18.580
0.2525	-4.360	26.290	-30.650
0.4325	-6.000	28.380	-34.380
0.4775	-8.500	29.640	-38.140

From Tables 4 to 8, it has been observed that the Nusselt number remains positive and increases with the increase of α , ε , M and R_e , but decreases with increase of ϕ in the frozen flow regime. Further the Nusselt number remains negative and decreases with the increase of α , M and R_e , but increases with the increase of ε and ϕ in the equilibrium flow regime.

Table - 4 Variation of Nusselt number for different values of ε in frozen flow and equilibrium flow regimes

t	ε	q_{w_0}	q_{w_1}	N_u
0.0175	0.01	2.018	-21.865	23.883
0.0175	0.02	2.019	-21.880	23.899
0.0175	0.03	2.020	-21.887	23.907
0.4775	0.01	-56.270	-29.740	-26.530
0.4775	0.02	-58.740	-32.820	-25.920
0.4775	0.03	-62.620	-38.840	-23.780

Table - 5 Variation of Nusselt number for different values of ϕ in frozen flow and equilibrium flow regimes

t	ϕ	q_{w_0}	q_{w_1}	N_u
0.0225	0.01	2.022	-19.07	21.092
0.0225	0.02	2.019	-19.04	21.059
0.0225	0.03	2.015	-19.01	21.025
0.4775	0.01	-4.800	31.74	-36.540
0.4775	0.02	-0.870	29.95	-30.820
0.4775	0.03	2.585	27.56	-24.975

Table – 6 Variation of Nusselt number for different values of M in frozen flow and equilibrium flow regimes

t	M	q_{w_0}	q_{w_1}	N_u
0.0225	1.0	2.021	-19.067	21.088
0.0225	2.0	2.022	-19.068	21.090
0.0225	3.0	2.025	-19.069	21.094
0.4775	1.0	2.595	28.415	-25.820
0.4775	2.0	-9.820	33.900	-43.720
0.4775	3.0	-11.800	35.740	-47.540

Table – 7 Variation of Nusselt number for different values of α in frozen flow and equilibrium flow regimes

t	α	q_{w_0}	q_{w_1}	N_u
0.0175	0.01	2.020	-19.07	21.090
0.0175	0.02	2.035	-19.27	21.305
0.0175	0.03	2.050	-19.47	21.520
0.4775	0.01	-4.800	23.87	-28.150
0.4775	0.02	-8.800	24.13	-32.930
0.4775	0.03	-9.000	25.27	-34.270

Table – 8 Variation of Nusselt number for different values of R_e in frozen flow and equilibrium flow regimes

t	R_e	q_{w_0}	q_{w_1}	N_u
0.0225	6.0	2.022	-19.069	21.091
0.0225	5.0	2.018	-19.028	21.046
0.0225	4.0	2.014	-18.988	21.002
0.4775	6.0	-5.270	29.610	-34.880
0.4775	5.0	-4.860	27.790	-32.650
0.4775	4.0	-3.520	25.380	-28.900

From Tables 9 to 13, the following observations have been made in the frozen flow regime. The skin friction at the lower plate remains positive and decreases with the increase of α and R_e , but increases with the increase of ε , ϕ and M . Similarly the skin friction at the upper plate remains negative and decreases with the increase of α , ε and R_e , but increases with the increase of ϕ and M .

Again from Tables 9 to 13, the following observations have been made in the equilibrium flow

regime. The skin friction at either of the plates is positive and increases with increase of ε . The skin friction at either of the plates remains positive and decreases at the lower plate, but increases at the upper plate with the increase of M . Skin friction increases at the lower plate, but decreases at the upper plate with the increase of R_e and back flow occurs at the lower plate. The skin friction increases at the lower plate, but decreases at the upper plate with the increase of ϕ . Skin friction decreases at the lower plate, but increases at the upper plate with increase of α .

Table – 9 Variation of Skin friction coefficients at different values of ε in frozen flow and equilibrium flow regimes

t	ε	C_{f_0}	C_{f_1}
0.0175	0.01	0.000819	-0.0175276
0.0175	0.02	0.000821	-0.0175315
0.0175	0.03	0.000824	-0.0175321
0.4775	0.01	0.000705	0.4513800
0.4775	0.02	0.001530	1.2980000
0.4775	0.03	0.223520	2.3840000

Table – 10 Variation of Skin friction coefficients at different values of ϕ in frozen flow and equilibrium flow regimes

t	ϕ	C_{f_0}	C_{f_1}
0.0225	0.01	0.000470	-0.018055
0.0225	0.02	0.000495	-0.018045
0.0225	0.03	0.000520	-0.018040
0.4775	0.01	0.000705	0.451380
0.4775	0.02	0.002580	0.013275
0.4775	0.03	0.002820	0.010670

Table – 11 Variation of Skin friction coefficients at different values of M in frozen flow and equilibrium flow regimes

t	M	C_{f_0}	C_{f_1}
0.0225	1.0	0.0004701	-0.0180670
0.0225	2.0	0.0004703	-0.0180603
0.0225	3.0	0.0004705	-0.0180540
0.4775	1.0	0.0028200	0.0105700
0.4775	2.0	0.0020950	0.0709200
0.4775	3.0	0.0007050	0.4513800

Table – 12 Variation of Skin friction coefficients at different values of α in frozen flow and equilibrium flow regimes

t	α	C_{f_0}	C_{f_1}
0.0175	0.01	0.000470	-0.018055
0.0175	0.02	0.000310	-0.018195
0.0175	0.03	0.000160	-0.018330
0.4775	0.01	-0.000705	0.451380
0.4775	0.02	-0.004350	0.925650
0.4775	0.03	-0.007980	1.351000

Table – 13 Variation of Skin friction coefficients at different values of R_e in frozen flow and equilibrium flow regimes

t	R_e	C_{f_0}	C_{f_1}
0.0225	6.0	0.0004705	-0.018054
0.0225	5.0	0.0005100	-0.018019
0.0225	4.0	0.0054850	-0.017983
0.4775	6.0	-0.0006350	0.448600
0.4775	5.0	-0.0007050	0.451380
0.4775	4.0	-0.0008200	0.453315

The increase in magnetic number M is to decrease the magnitude of fluid as well as particle velocities (Figures 1 & 2), whereas the fluid and particle temperature increase (Figures 3 & 4) throughout the flow regime.

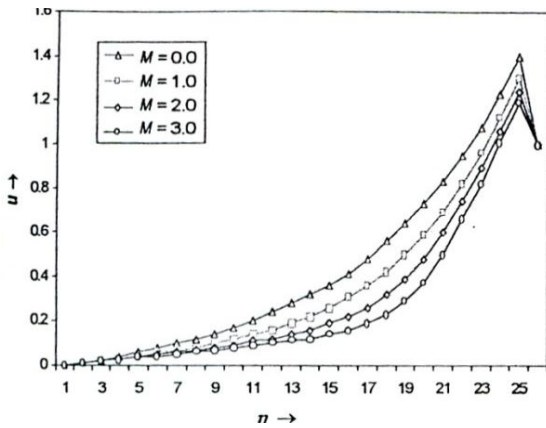


Figure 1 Velocity profile u for the fluid phase at different values of M

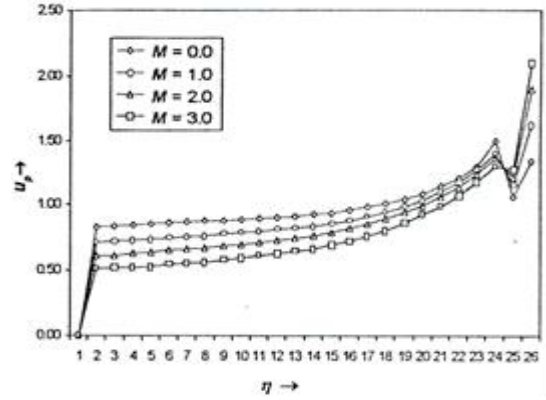


Figure 2 Velocity profile u_p for the particle phase at different values of M

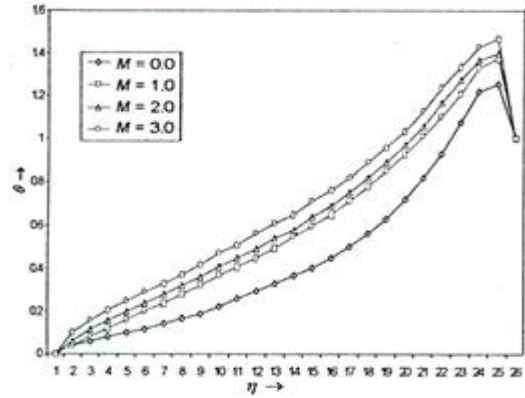


Figure 3 Temperature profile θ for the fluid phase at different values of M

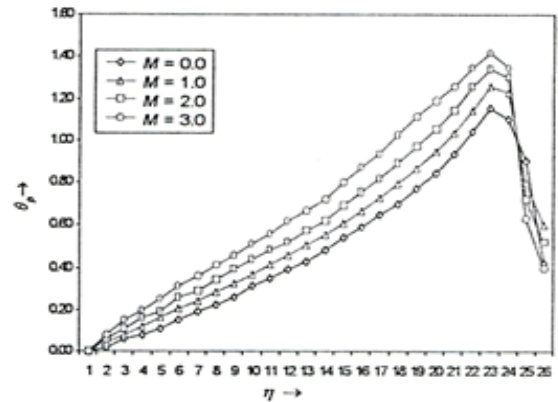


Figure 4 Temperature profile θ_p for the particle phase at different values of M

The fluid and particle velocities become oscillatory for large values of diffusion parameter ε

(Figures 5 & 6). The fluid temperature increases with the increase of diffusion parameter ε (Figure 7), but the particle temperature becomes oscillatory for large diffusion parameter ε (Figure 8).

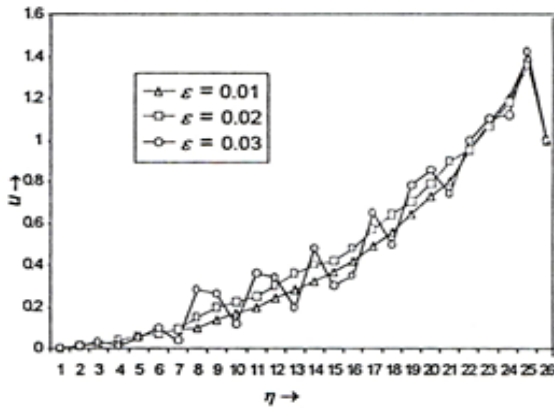


Figure 5 Velocity profile u for the fluid phase at different values of ε

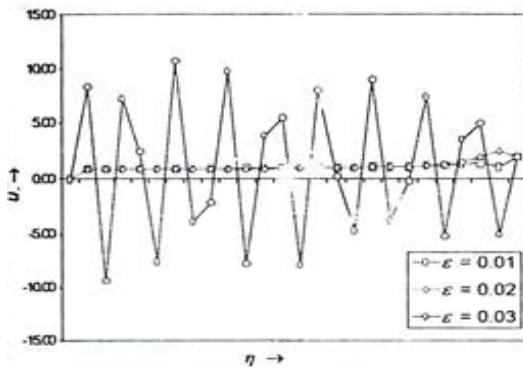


Figure 6 Velocity profile u_p for the particle phase at different values of ε

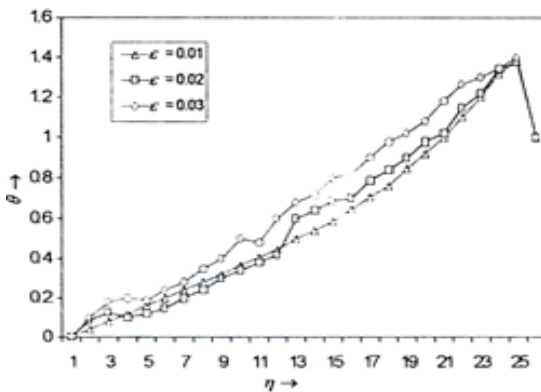


Figure 7 Temperature profile θ for the fluid phase at different values of ε

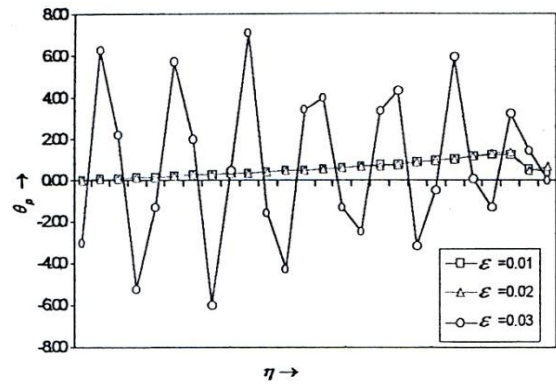


Figure 8 Temperature profile θ_p for the particle phase at different values of ε

The effect of concentration parameter α on fluid velocity is to decrease near the lower plate and to increase towards the upper plate (Figure 9). But the particle velocity decreases as concentration parameter α increases (Figure 10). The temperature of both the fluid and particles increase with the increase of concentration α of particles (Figures 11 & 12).

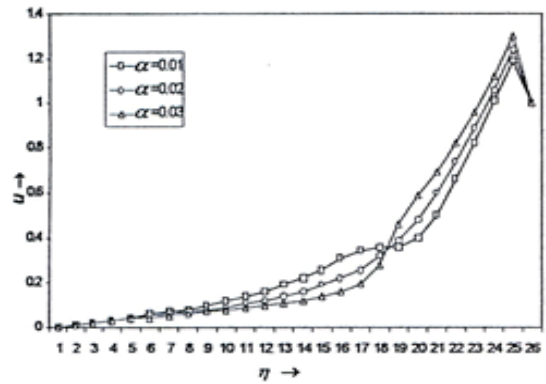


Figure 9 Velocity profile u for the fluid phase at different values of α

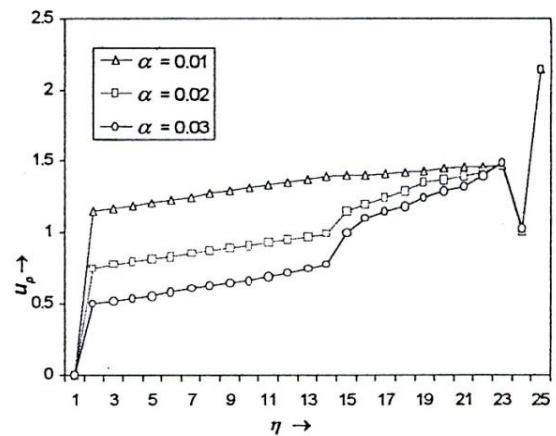


Figure 10 Velocity profile u_p for the particle phase at different values of α

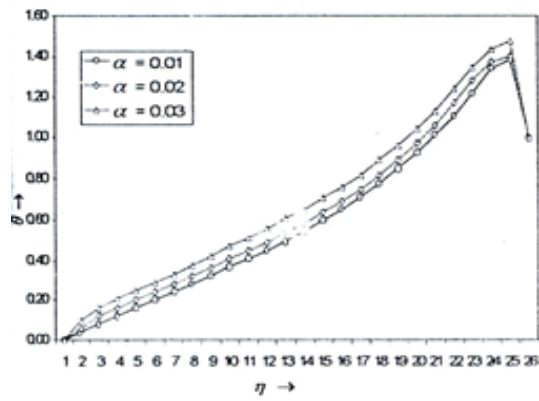


Figure 11 Temperature profile θ for the fluid phase at different values of α

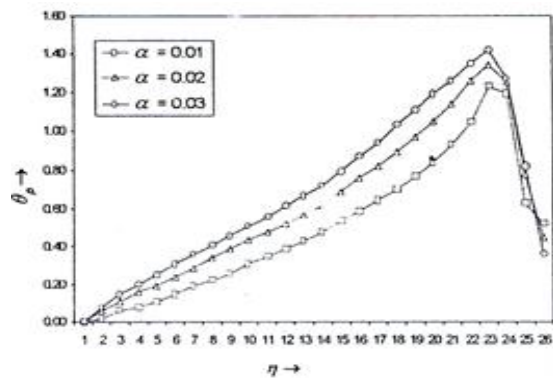


Figure 12 Temperature profile θ_p for the particle phase at different values of α

The fluid velocity increases with increase of volume fraction ϕ of the particles whereas the particle velocity shows a decreasing trend (Figures 13 & 14). The fluid and particle temperature decrease near the lower plate and increase towards the upper plate with increase of volume fraction ϕ (Figures 15 & 16).

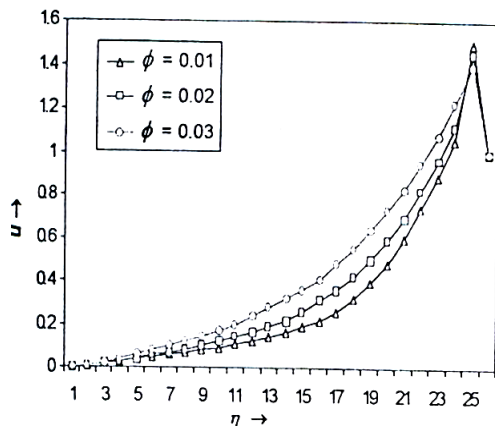


Figure 13 Velocity profile u for the fluid phase at different values of ϕ

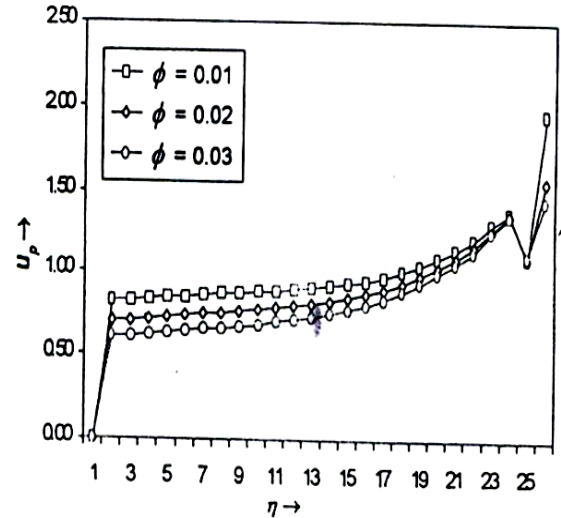


Figure 14 Velocity profile u_p for the particle phase at different values of ϕ

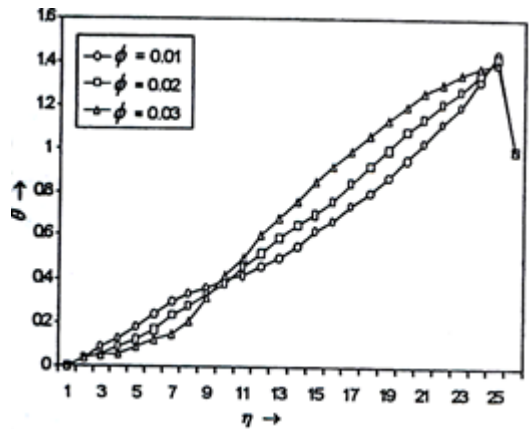


Figure 15 Temperature profile θ for the fluid phase at different values of ϕ

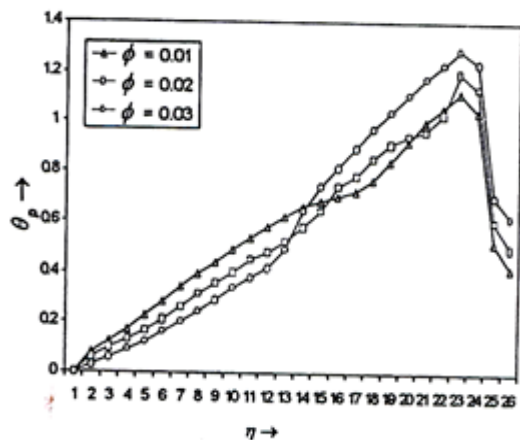


Figure 16 Temperature profile θ_p for the particle phase at different values of ϕ

REFERENCES

- [1] Saffman P.G., On the stability of a laminar flow of a dusty gas, *J. Fluid Mech.* 13, 1962, pp. 120-128
- [2] Michael D.H., and Miller D.A., Plane parallel flow of a dusty gas, *Mathematika* 13, 1966, pp. 97-109
- [3] Baral M.C., Plane parallel flow of conducting dusty gas, *Jou. Phy. Soc. of Japan* 25, 1968, pp. 1701-1702
- [4] Jana R.N., and Datta N., Couette flow and Heat Transfer in a Rotating System, *Acta Mechanica*, 1977, pp.301-306
- [5] Nag S. K., Jana R. N., and Datta N., Couette flow of a dusty gas, *Acta Mechanica*, 33, 1979, pp.179-187
- [6] Mitra P., and Bhattacharyya P., Unsteady hydro magnetic laminar flow of a conducting dusty fluid between two parallel plates started impulsively from rest, *Acta Mech.* 39, 1981, pp. 171
- [7] Datta N., and Mishra S.K., Unsteady Couette flow and Heat transfer in a dusty gas, *Int. Comm. Heat Mass Transfer*, Vol. 10, 1983, pp.153-162
- [8] Datta N., and Mishra S.K., Couette flow of a dusty fluid in a Rotating Frame of Reference, *Jour. Math. Phy. Sci.*, Vol. 22, No. 3, 1988
- [9] Aboul-Hassan L., Sharaf El-Din H., and Megahed A.A., Temperature distribution in a dusty conducting fluid flowing through two parallel infinite plates due to the motion of one of them, in: *First International Conference of Engineering Mathematics and Physics*, Cairo, 1991, pp. 723-734
- [10] Panda T.C., Mishra S.K., and Panda K.Ch., Volume fraction and diffusion analysis in SPM modelling in an inertial frame of reference, *Acta Ciencia Indica*, Vol. XXVII, No. 4, 2001, pp. 515-525
- [11] Attia H. A., Unsteady MHD couette flow and heat transfer of dusty fluid with variable physical properties, *Applied Mathematics and Computation*, Volume 177, Issue 1, 2006, pp. 308 – 318
- [12] Govindarajan A. , Ramamurthy V., and Sundarammal K., 3D couette flow of dusty fluid with transpiration cooling, *Journal of Zhejiang University SCIENCE A*, 8(2), 2007, pp. 313-322
- [13] Giresha B.J., Bagewadi C.S., and Venkatesh P., Unsteady flow of a conducting dusty fluid between two parallel plates, *Applied Sciences*, Vol. 9, 2007, pp.102-108
- [14] Attia H. A., Unsteady hydromagnetic Couette flow of dusty fluid with temperature dependent viscosity and thermal conductivity under exponential decaying pressure gradient, *Communications in Nonlinear Science and Numerical Simulation*, Volume 13, Issue 6, 2008, pp.1077-1088
- [15] Eguía P. , Zueco J., Granada E. ,and Patiño D. , NSM solution for unsteady MHD Couette flow of a dusty conducting fluid with variable viscosity and electric conductivity, *Applied Mathematical Modelling*, Volume 35, Issue 1, 2011, pp. 303-316
- [16] Loeb L.B., *Static Electrification*. Springer-Verlag, Berlin, Germany and New York, 1958
- [17] Soo S.L., Effect of electrification on the dynamics of a particulate system, *I and EC Fund.* 3, 1964, pp.75-80